Journal of Sound and Vibration (1999) **228**(5), 1079–1102
Article No. jsvi.1999.2460, available online at http://www.idealibrary.com on IDEAL®

USING FAST VIBRATIONS TO QUENCH FRICTION-INDUCED OSCILLATIONS

J. J. THOMSEN

Department of Solid Mechanics, Technical University of Denmark, DK-2800 Lyngby, Denmark

(*Received* 6 *May* 1999, *and in final form* 14 *June* 1999)

This work examines how friction-induced self-excited oscillations are affected by high-frequency external excitation. Simple analytical approximations are derived for predicting the occurrence of self-excited oscillations for the traditional mass-on-moving-belt model—with and without high-frequency excitation. It appears that high-frequency excitation can effectively cancel the negative slope in the friction–velocity relationship, and may thus present self-excited oscillations. To accomplish this, it is sufficient that the (non-dimensional) product of excitation amplitude and frequency exceeds the velocity corresponding to the minimum kinetic coefficient of friction. Simple expressions are also given for predicting the excitation necessary for quenching self-excited oscillations at or below a specified belt velocity. These and other results contribute to the general understanding of how friction properties may change under the action of fast vibrations.

1. INTRODUCTION

Dry friction can induce self-excited oscillations in mechanical systems with sliding components. This paper considers how such vibrations are changed in the presence of high-frequency external excitation. Simple analytical expressions are provided for predicting how high-frequency excitation can reduce or totally suppress friction-induced vibrations.

Many sliding mechanical interfaces are characterized by some form of dry friction, with a force–velocity curve having negative slope at low velocities. Then friction drops off as the contacting object starts to move, whereas at higher velocities the friction force increases again. The negative slope corresponds to negative damping, and may thus cause oscillations that grow in amplitude, until a balance of dissipated and induced energy is reached (Lord Rayleigh knew this; see reference [1, Vol. I, p. 212]). Typically there are two phases of such oscillations: a *stick phase* with no slippage between parts and friction forces limited by static friction, followed by a *slip* phase with a somewhat lower friction force. Since these oscillations occur without any external periodic input, they are called *self-excited*. There are sources of self-excited oscillations other than dry friction, e.g., fluid or gas flowing inside or along structures causing flutter or galloping vibrations [2], but they are not considered here.

0022-460X/99/501079 + 24 $30.00/0

Friction-induced oscillations may occasionally provide pleasant sensations, such as the singing from bowed violin strings. However, more often they are quite annoying (e.g., as squeaking door hinges) and can even present serious environmental problems. For example, the squeal from activated drum brakes in buses and trucks daily puts significant stress on drivers and inhabitants in city areas [3], as do the unpleasant sound from trains that brake or pass curved tracks. And the occasional chatter experienced with friction clutches, friction belts, and machine tools may obstruct proper operation of these devices and provide discomfort to the operator.

A number of works have been devoted to the study of friction-induced oscillations. For ease of set-up and interpretation an idealized physical system consisting of a mass sliding on a moving belt has been considered very often, as in the case of the present study. Panovko and Gubanova [4] describe how stable self-excited oscillations can occur only with non-linear systems, since for linear systems unattenuated oscillations can be maintained only if there is a periodical external input. For a system similar to the mass-on-moving-belt with a friction characteristic having minimum coefficient at velocity v_m, it showed that self-excited oscillations occur only when the velocity of the belt is lower than v_m. Tondl [5], Nayfeh and Mook [6], and Mitropolskii and Nguyen [7] describe self-excited oscillations of the mass-on-belt system, presenting approximate expressions for the vibration amplitudes for the case where there is no sticking between mass and belt. Popp [8] presents models and numerical and experimental results for four systems that are similar to the mass-on-moving-belt.

Yokoi and Nakai [9, 10] studied friction-induced squeal noise for an experimental rod pressed against a rotating disk (equivalent to the mass-on belt system). Experiments showed that sequel occurred at a natural frequency of the system, increasing in sound level as surfaces are worn and as the coefficient of friction increases. Experimentally measured friction–velocity curves showed negative slope, until some sliding velocity v_m at which it turned positive.

Ibrahim [11, 12] presents and discusses the basic mechanics of friction and friction models, and provides a review of the literature on the topic. McMillan [13] provides a similar, more recent review, and suggests more advanced friction models for reproducing hysteresis and other phenomena that are not captured by simpler models.

Popp *et al.* [14] describe how is engineering applications stick–slip vibrations are undesired and should be avoided, since they affect precision of motion and safety of operation, and create noise. They present a numerical bifurcation analysis of a mass-on-belt system subjected to near-resonant external excitation. Hinrichs *et al.* [15] too present a numerical analysis of this system, and contribute with experimental results and a suggestion for a more advanced friction model with a stochastic component. Elmer [16] discusses stick–slip and pure-slip oscillations of the mass-on-belt system with no damping and different kinds of friction functions, and provides analytical expressions for the transfer between stick–slip and pure-slip oscillations.

This present work differs from those mentioned above in including external periodic excitation of high frequency (far beyond resonance) and small amplitude.

The basic question to be examined is how this excitation affects the presence and characteristics of self-excited oscillations. It is already known that fast vibrations can effectively turn classical Coulomb friction (with piece-wise constant coefficient of friction) into viscous-like damping [17]. This study then examines the effect of high-frequency excitation for systems having friction characteristics with a negative slope in the force–velocity relationship, that is, systems that are prone to friction-induced self-excited vibrations.

As for methods to quench or reduce friction-induced vibrations, it is a common experience, that oil or grease works well. Lubrication has the effect of changing the dominating mechanism of energy dissipation from dry friction into viscous-like damping. Since viscous damping does not have a negative slope in its force–velocity characteristic, self-excited oscillations cannot occur by that mechanism. While oil may stop a rusty door hinge from squeaking, this cure is inadequate for cases where dry friction is necessary for proper operation of a device (e.g., vehicle brakes). The problem here is that once the lubrication has been applied, it cannot be quickly removed. Similar problems may arise when using the basic techniques described by Tondl [5]: the traditional tuned mass damper (TMD), and visco-elastically mounted foundation mass. Both of these permanently change the dynamical properties of the system they are supposed to damp. Fast vibrations, as described in the present work, might provide a more flexible alternative. In effect, it corresponds to a form of lubrication that can be controlled and removed very quickly by changing amplitude or frequency of the excitation.

Section 2 of the paper presents the model, and some typical responses with and without fast harmonic excitation. Section 3 provides analytical predictions of friction-induced oscillations when there is no harmonic excitation, and section 4 similarly for the case of fast harmonic excitation. These results are used in section 5 to provide simple analytical criteria for quenching friction-induced oscillations by using fast vibrations.

2. THE MODEL SYSTEM

2.1. EQUATION OF MOTION

Figure 1 shows the system: a mass M on a belt that moves at constant speed V_b. The mass is a rigid body with characteristic length L, at time t having position $X(t)$

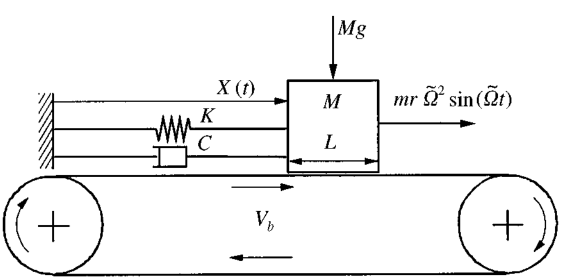

Figure 1. The system: a mass at position $X(t)$ on a belt that moves at constant speed V_b.

in a fixed frame of coordinates. It is subjected to gravity loading Mg, linear spring-loading KX, damping force $C\mathrm{d}X/\mathrm{d}t$, and a Coulomb friction force $Mg\mu(V_r)$ where μ is the friction force as a function of the relative velocity between mass and belt, $V_r = \mathrm{d}X/\mathrm{d}t - V_b$. Further there is an external time harmonic loading of frequency $\tilde{\Omega}$ and amplitude $mr\tilde{\Omega}^2$ (e.g., this load could arise from a horizontally unbalanced mass m at eccentricity r running at angular speed $\tilde{\Omega}$).

The equation of motion is, in non-dimensional form:

$$\ddot{x} + 2\beta\dot{x} + x + \gamma^2\mu(\dot{x} - v_b) = a\Omega^2 \sin(\Omega\tau), \tag{1}$$

where $\dot{x} = \mathrm{d}x/\mathrm{d}\tau$ is the non-dimensional velocity of the mass at non-dimensional time τ, and

$$\begin{gathered}\tau = \omega_0 t, \qquad \omega_0^2 = \frac{k}{m}, \qquad x = \frac{X}{L}, \\ \gamma^2 = \frac{g/L}{K/M}, \qquad 2\beta = \frac{C}{\sqrt{KM}}, \qquad a = \frac{m}{M}\frac{r}{L}, \qquad v_b = \frac{V_b}{\omega_0 L}, \qquad \Omega = \frac{\tilde{\Omega}}{\omega_0}.\end{gathered} \tag{2}$$

Here lengths have been normalized by the characteristic length L and time by the linear natural frequency ω_0 for free oscillations of the mass when there is no damping and friction. Then γ^2 describes the ratio of gravity loading to spring force, β the damping ratio (actual to critical), v_b the speed of the belt, Ω the frequency of the harmonic excitation, and a the kinematic amplitude of the excitation.

Alternatively, multiplying by $\dot{x}$ and integrating over time, one can express (1) in the form of a balance of changing energies:

$$\frac{\mathrm{d}}{\mathrm{d}\tau}(E_{kin} + E_{pot}) = \frac{\mathrm{d}}{\mathrm{d}\tau}(E_{inp} - E_{dis}), \tag{3}$$

where the non-dimensional energies (kinetic, potential, input, and dissipated) are given by

$$\begin{aligned} E_{kin} &= \tfrac{1}{2}\dot{x}^2; \qquad E_{pot} = \tfrac{1}{2}x^2, \\ E_{inp} &= \int a\Omega^2 \dot{x} \sin(\Omega\tau)\,\mathrm{d}\tau, \\ E_{dis} &= \int (2\beta\dot{x}^2 + \gamma^2 \dot{x}\mu(\dot{x} - v_b))\,\mathrm{d}\tau \end{aligned} \tag{4}$$

and the corresponding dimensional energies are obtained by multiplying by kL^2.

2.2. FRICTION FUNCTION

For the friction function μ we assume, as in reference [4]

$$\mu(v_r) = \mu_s \operatorname{sgn}(v_r) - \tfrac{3}{2}(\mu_s - \mu_m)\left(\frac{v_r}{v_m} - \frac{1}{3}\left(\frac{v_r}{v_m}\right)^3\right), \tag{5}$$

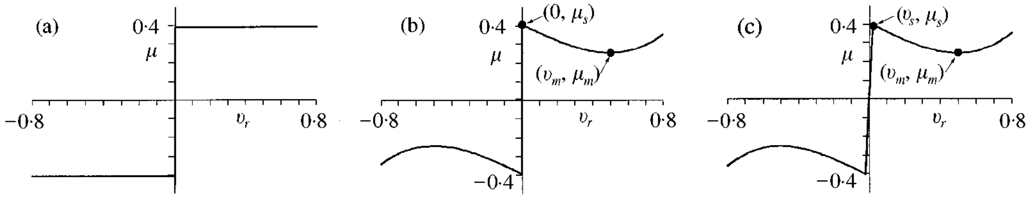

Figure 2. Friction functions as given by equation (5) or equation (6) with $\mu_s = 0{\cdot}4$ and $v_m = 0{\cdot}5$. (a) Simple Coulomb friction ($\mu_m = \mu_s$, $v_s = 0$); (b) negative-slope friction $\mu_m = 0{\cdot}25$, $v_s = 0$); (c) the same as figure (b) except $v_s = 0{\cdot}02$.

where $v_r = \dot{x} - v_b$ is the (non-dimensional) relative velocity between mass and belt, μ_s is the coefficient of static friction, and v_m is the velocity corresponding to the minimum coefficient μ_m of kinetic friction, $\mu_m \leqslant \mu_s$. Thus the function satisfies $|\mu(0)| \leqslant \mu_s$, $\mu(v_m) = \mu_m$, $\mathrm{d}\mu/\mathrm{d}v_r = 0$ for $v_r = v_m$, and $\mu(-v_r) = -\mu(v_r)$. Figure 2(a) depicts this function for the case $\mu_m = \mu_s$, which corresponds to simple Coulomb friction. Figure 2(b) depicts the function for typical parameter values (v_m, μ_m, μ_s) to be used in this study. It appears that $|\mu| \leqslant \mu_s$ when the mass is at rest on the moving belt ($v_r = 0$, *stick phase*), whereas when the mass starts sliding the friction forces initially decreases with increasing velocity ($v_r \neq 0$, *slip phase*).

For numerical integration of equation (1) the jump discontinuity of equation (5) at $v_r = 0$ causes slow convergence and numerical stability problems. This can be cured by using, instead of equation (5)

$$\mu(v_r) = \begin{cases} \mu_s\, v_r/v_s & \text{for } |v_r| < v_s, \\ \operatorname{sgn}(v_r)\left[u_s - \frac{3}{2}(\mu_s - \mu_m)\left(\dfrac{|v_r| - v_s}{v_m - v_s} - \dfrac{1}{3}\left(\dfrac{|v_r| - v_s}{v_m - v_s}\right)^3\right)\right] & \text{for } |v_r| \geqslant v_s \end{cases} \tag{6}$$

with a very small number for v_s, e.g. 10^{-4}. This function is similar to equation (5), except that it satisfies $\mu(0) = 0$ and $\mu(\pm v_s) = \pm \mu_s$. Figure 2(c) depicts this function for a rather large value of v_s, just to illustrate the effect of finite-valued v_s. For small values of v_s the function looks as the one in Figure 2(b), and the results of numerical integration are indistinguishable from those obtained by using $v_s = 0$. Then we consider very slow motions $|v_r| < v_s$ as effectively "sticking". Expression (6) will be used for numerical integration, whereas for analytical development we use equation (5). (An anonymous reviewer points out that equation (6) could be replaced by a smooth function, by combining a polynomial function of v_r with $\arctan(kv_r)$, $k \gg 1$; this technique is used e.g., in references [14, 18].)

2.3. TYPICAL RESPONSES

We here illustrate typical responses of the system as obtained by numerical integration fifth and sixth order variable step-size Runge–Kutta) of the equation of motion (1) with initial conditions $x(0) = \dot{x}(0) = 0$ and $v_s = 10^{-4}$ (no difference in results for $v_s \leqslant 10^{-4}$, but slower convergence). The friction function μ is given by

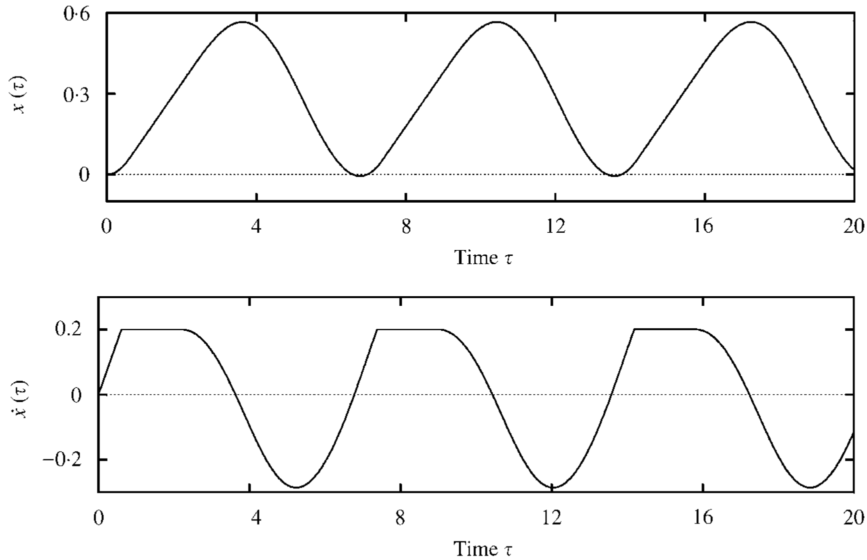

Figure 3. Displacement and velocity responses $x(\tau)$ and $\dot{x}(\tau)$ without fast excitation. Numerical integration of equation (1) with $v_b = 0{\cdot}2$, $\gamma^2 = 1$, $\beta = 0{\cdot}05$, $v_m = 0{\cdot}5$, $\mu_m = 0{\cdot}25$, $v_s = 10^{-4}$, $\mu_s = 0{\cdot}4$, $a = 0$. Self-excited oscillation grow up and stabilize (for small β they will do so for $v_b < v_m$).

equation (6) with parameters corresponding to the typical case of initially negative slope, i.e. Figure 2(b) and 2(c).

Figure 3 show the time-varying position $x(\tau)$ of the mass when there is no external harmonic excitation, i.e., $a = 0$. Self-excited oscillations grow up and stabilize. As shown below, for small damping β this will occur whenever the velocity of the belt is lower than the velocity of minimum friction coefficient, $v_b < v_m$. This is quite natural, since for $v_b > v_m$ motion occurs at conditions where friction forces increase with velocity, and so, should the mass start to move faster than i.e., it will be met by opposing forces. From the velocity response it appears there are intervals of stick ($\dot{x}(\tau) = \text{constant} = v_b$), each lasting until the restoring spring force exceeds the maximum attainable friction force, and the mass starts to slide ($\dot{x}(\tau) < v_b$). This phenomenon is well understood and described (see e.g., references [4–8, 14, 15]).

Figure 4 shows similar responses obtained when adding high-frequency harmonic excitation of very small amplitude ($\Omega = 50$, $a = 0{\cdot}01$). As observed this prevents self-excited oscillations from building up. However, the mass performs tiny oscillations at the excitation frequency about a non-zero equilibrium. The presence of fast vibrations effectively smoothens out the discontinuity of the dry friction characteristic, as will be shown in section 4. This tends to cancel the negative slope of the characteristic, and thereby prevents self-excited oscillations from building up. The smoothening effect itself is well described (see e.g., reference [17]), and is in fact utilized in many industrial processes, e.g. vibrational piling. However, there seems to be no theoretical basis for describing this effect with negative-slope frictional characteristics and self-excited oscillations. We shall provide this below.

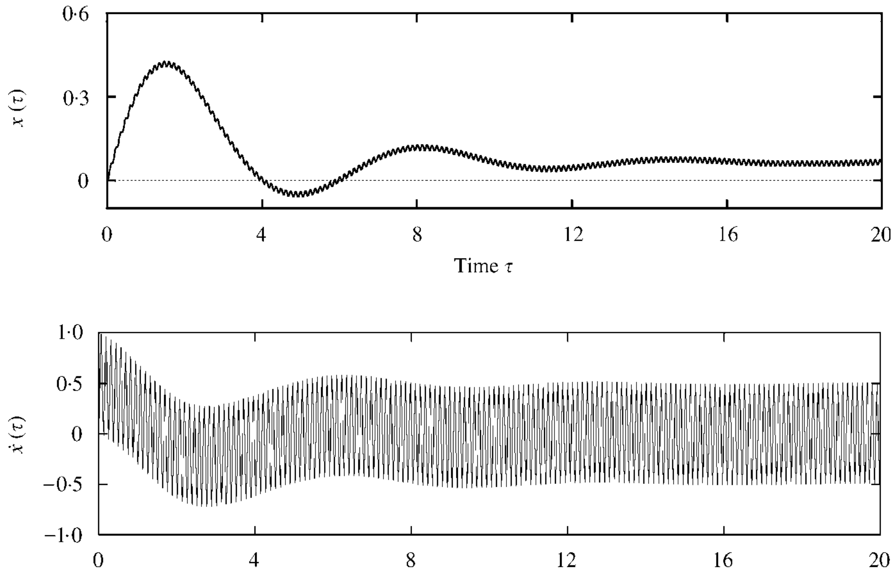

Figure 4. Responses in the presence of high-frequency external excitation. Numerical integration of equation (1) with parameters as for Figures 3, except $\Omega = 50$, $a = 0{\cdot}01$. The fast excitation quenches self-excited oscillations.

3. SELF-EXCITED OSCILLATIONS: CASE OF *NO* HARMONIC EXCITATION

Here the occurrence and character of self-excited oscillations for the system when there is no harmonic excitation is considered and then in section 4 consideration is given to how fast harmonic excitation affects such oscillations.

How large are the amplitudes of friction-induced self-excited oscillations? Apparently, analytical predictions have been given only for the amplitudes of self-excited oscillations without sticking motions (where standard perturbation analysis can be applied, e.g. references [4–7]). However, as shown below, such motions typically occur only for a rather narrow range of belt velocities. Therefore, this section describes in some depth the development of approximate expressions for predicting which type of self-excited vibrations (with or without stick) will occur under given circumstances, and what their amplitudes are.

3.1. TYPES OF MOTION

When there is no harmonic excitation ($a = 0$) equation (1) has a static equilibrium at $x = \bar{x}$,

$$\bar{x} = -\gamma^2 \mu(-v_b) = \gamma^2 \mu(v_b), \tag{7}$$

since then $\dot{x} = \ddot{x} = 0$. At certain conditions this equilibrium can turn unstable, and the system will perform periodic oscillations about it. To study such motions the origin is shifted to describe motions $u(\tau) = x(\tau) - \bar{x}$ near the equilibrium. Inserting into equation (1) one finds

$$\ddot{u} + u + \varepsilon h(\dot{u}) = 0, \tag{8}$$

where $\dot{u} = \mathrm{d}u/\mathrm{d}\tau$ and

$$\varepsilon h(\dot{u}) \equiv 2\beta\dot{u} + \gamma^2(\mu(\dot{u} - v_b) - \mu(-v_b)). \tag{9}$$

Here $\varepsilon \ll 1$ has been introduced merely as a book-keeping parameter to indicate that damping and friction terms are assumed small compared to stiffness and inertia. This is fulfilled when β and η are small quantities, where η defines the *friction difference*:

$$\eta \equiv \tfrac{3}{2}\gamma^2(\mu_s - \mu_m)/v_m. \tag{10}$$

The equilibrium $u = \dot{u} = 0$ of this system corresponds to a state of constant sliding, with the mass in Figure 1 being at rest with respect to the fixed frame and the belt sliding at constant velocity v_b below it. This state can be stable or unstable. If it is unstable, then stable periodic motion takes over; this is the only possibility, since generally the steady state must be either statical equilibrium, periodic motion, or chaotic motion—and chaotic solutions cannot occur for second order autonomous ordinary differential equations (e.g. reference [19]).

Two different kinds of periodic solutions to equation (8) are considered: *pure-slip oscillations*, where $\dot{u}(\tau) < v_b$ at all times, i.e., the mass never overhauls the belt—and *stick–slip oscillations* where $\dot{u}(\tau) \leqslant v_b$; i.e., the mass occasionally sticks to the belt (as in Figure 3). They are dealt with separately below.

3.2. PURE-SLIP PERIODIC MOTIONS

Using standard averaging (e.g. references [6, 7, 19]) for equation (8), a Van der Pol transformations first applied

$$\begin{aligned} u &= A\sin\psi, \\ \dot{u} &= A\cos\psi; \qquad \psi(\tau) \equiv \tau + \theta(\tau), \end{aligned} \tag{11}$$

where $A(\tau)$ and $\theta(\tau)$ are unknown functions to be determined, and $\dot{A}\sin\psi + A\dot{\theta}\cos\psi = 0$ by definition of the transform. The transform recasts equation (8) into two first order differential equations governing $A(\tau)$ and $\theta(\tau)$:

$$\begin{aligned} \dot{A} &= -\varepsilon h(A\cos\psi)\cos\psi, \\ A\dot{\theta} &= \varepsilon h(A\cos\psi)\sin\psi. \end{aligned} \tag{12}$$

Since $\varepsilon \ll 1$ the right-hand terms are small so that $\dot{A}$ and $\dot{\theta}$ are small, that is, A and θ change only little during one period of the oscillating terms $\sin\psi$ and $\cos\psi$. Thus, for determining $A(\tau)$ and $\theta(\tau)$ approximately one can average the right-hand sides of equations (12) over one period, considering A and θ to be constant during the (short) period of integration, i.e., approximately:

$$\dot{A} = -\frac{\varepsilon}{2\pi}\int_0^{2\pi} h(A\cos\psi)\cos\psi\,\mathrm{d}\psi,$$
$$A\dot{\theta} = \frac{\varepsilon}{2\pi}\int_0^{2\pi} h(A\cos\psi)\sin\psi\,\mathrm{d}\psi. \tag{13}$$

Now assume the function h to be given as a cubic polynomial (or truncated Taylor expansion) with constant coefficients h_i:

$$h(\dot{u}) = h_0 + h_1\dot{u} + h_2\dot{u}^2 + h_3\dot{u}^3. \tag{14}$$

Then the averaged equations (13) becomes

$$\dot{A} = -\tfrac{1}{2}\varepsilon A(h_1 + \tfrac{3}{4}h_3A^2),$$
$$A\dot{\theta} = 0. \tag{15}$$

There are two equilibriums, defined by $\dot{A} = \dot{\theta} = 0$, for these equations (corresponding to stationary solutions as $\tau \to \infty$): A trivial one $A(\tau) = 0$, corresponding to the statical equilibrium $u(\tau) = 0$, and a non-trivial solution given by

$$A(\tau) = A_0 \equiv \sqrt{-\tfrac{4}{3}h_1/h_3},$$
$$\theta(\tau) = \theta_0 = \text{constant} \quad \text{for } \tau \to \infty \tag{16}$$

corresponding to periodic solutions $u(\tau) = A_0\sin(\tau + \theta_0)$.

A particular solution is unstable if $\partial\dot{A}/\partial A$ is positive, and otherwise stable. Using this with equations (15) and (16) one finds that the statical equilibrium $u = 0$ becomes unstable when $h_1 < 0$, that is, when the function $h(\dot{u})$ has negative slope at $\dot{u} = 0$. If this is the case, and if $h_3 > 0$, then the periodic solution $u = A_0\sin(\tau + \theta_0)$ exists and is stable. Hence for $h_3 > 0$ the statical equilibrium undergoes a supercritical Hopf-bifurcation across the bifurcation value $h_1 = 0$.

Using equation (9) to compute the slope of $h(\dot{u})$ and utilizing that $\mu(-v_r) = -\mu(v_r)$, it is found that the equilibrium $u = 0$ becomes unstable when

$$\mu'(v_b) + 2\beta/\gamma^2 < 0, \tag{17}$$

where $\mu' \equiv \mathrm{d}\mu/\mathrm{d}v_r$. That is, when there is no damping ($\beta = 0$), then the equilibrium becomes unstable when the friction function $\mu(v_r)$ has negative slope at the belt velocity v_b, and damping tends to stabilize the equilibrium.

For the particular friction function of this study one finds, inserting equation (5) with the assumption $\dot{u} < v_b$ into equation (9) and rearranging, that $h(\dot{u})$ has the form (14) with the following coefficients:

$$h_0 = 0, \qquad h_1 = 2\beta - \eta(1-(v_b/v_m)^2), \qquad h_2 = -\,\eta v_b/v_m^2, \qquad h_3 = \tfrac{1}{3}\eta/v_m^2, \quad (18)$$

where η is defined by equation (10). Hence $u = 0$ is unstable ($h_1 < 0$) when

$$v_b < v_{b1} \equiv v_m\sqrt{1 - 2\beta/\eta}. \qquad (19)$$

As observed, when there is no viscous damping ($\beta = 0$) the static equilibrium is unstable whenever the velocity of the belt is lower than the velocity v_m corresponding to the mimimum coefficient of friction. Viscous damping tends to stabilize the static equilibrium, giving a positive contribution to the slope h_1, and decreasing the unstable range of belt velocities v_b. At sufficiently large damping, $2\beta > \eta$, the static equilibrium is always stable and there is no periodic motion since, then, $h_1 > 0$ for all v_b.

As mentioned above, periodic motions exist and are stable when $h_1 < 0$ (i.e., when the static equilibrium is unstable) *and* $h_3 > 0$. Since $\mu_s > \mu_m$ the latter requirement is automatically fulfilled. The amplitude A_0 of the stable periodic motion is found by inserting equation (18) into equation (16) and using equation (19) to give

$$A_0 = 2v_m\sqrt{1-(v_b/v_m)^2 - 2\beta/\eta} = 2\sqrt{v_{b1}^2 - v_b^2}, \quad v_{b0} < v_b < v_{b1}, \qquad (20)$$

where v_{b1} is the belt velocity where pure-slip oscillations first occur, as given by equation (19).

Since equation (20) assumes pure slip, i.e., no sticking, the increase in amplitude for decreasing v_b will cease when the mass starts sticking to the belt, i.e., when $\max(\dot{u}) = v_b$. Since $\max(\dot{u}) = A_0$ (by equations (11) and (16)), it is found that sticking first occurs when $A_0 = v_b$. Inserting this into equation (20) and solving for v_b we find that stick–slip oscillations occur when $v_b < v_{b0}$ where

$$v_{b0} = \sqrt{\tfrac{4}{3}}\, v_{b1}. \qquad (21)$$

Hence, the range of belt velocities where pure-slip oscillations occur is rather small, its width $(v_{b1} - v_{b0})$ being only $1 - \sqrt{4/5} \approx 10\%$ of v_{b1}. It forms a transition zone to a wider range of belt velocities where stick–slip motions occur.

When sticking has just started, the amplitude of oscillations is given by inserting $v_b = v_{b0}$ in equation (20), and then equations (19) and (21) are used to find

$$A_0|_{v_b = v_{b0}} = A_{0,\max} = v_{b0} = \sqrt{\tfrac{4}{5}}\, v_m\sqrt{1 - 2\beta/\eta}, \qquad (22)$$

where it should be noted that η depends on v_m (cf. equation (10)). Hence, for vanishing damping β the maximum amplitude grows linearly with the velocity v_m of minimum kinetic friction.

Results similar to those given by equations (16) and (17) can be found elsewhere, e.g. references [4–7]. However, these studies are limited strictly to predicting pure-slip oscillations, and thus do not provide the results given by equation (20) and on. In particular, no mention seems to be made of the result obtained here, that pure-slip oscillations may occur only for a rather narrow range of belt velocities. This range may even vanish for certain types of friction functions. For example, if the cubical velocity term in equation (5) is replaced by a quadratic, the friction function will still resemble the one in Figure 2(b), and the condition for the statical equilibrium to be unstable will not change. However, one can show that quadratic terms cannot limit the growth in unstable oscillation amplitudes (i.e. $A_0 \to \infty$ in equation (16)), so that stable pure-slip oscillations cannot exist and all self-excited oscillations will be of the stick–slip type. Therefore, to be of any practical value, this present study must include consideration to stick–slip oscillations.

3.3. STICK–SLIP OSCILLATIONS

Now assume that $v_b < v_{b0}$, i.e., during part of the oscillation period the velocity of the mass equals the velocity of the belt, $v_r = \dot{x} - v_b = \dot{u} - v_b = 0$. With stick–slip oscillations the averaging procedure used above for pure-slip oscillations cannot be readily employed. This is because the friction characteristics (5) cannot be Taylor-expanded near $v_r = 0$ (the pure-slip analysis assumes $v_r < 0$ strictly for all τ). However, it is possible to analyze the stick and the slip phases of the motion separately, and tie the results together to obtain an approximate expression for the oscillation amplitude.

We begin by assuming that after a period of slip ($\dot{x} < v_b$) the mass has just started to stick at time $\tau = \tau_0$ so that $\dot{x}(\tau_0) = v_b$. Then the position of the mass will increase linearly with time as long as the mass continuous to stick, that is

$$x(\tau) = x(\tau_0) + (\tau - \tau_0)v_b, \quad \tau \in [\tau_0;\tau_1], \tag{23}$$

where τ_1 is the time at which sticking stops and the mass again starts to slip. With stick one has $\dot{x} = v_b$ and $\ddot{x} = 0$, so that the equation of motion (1) (with $a = 0$) becomes

$$2\beta v_b + x + \gamma^2 \mu(0) = 0, \quad \tau \in [\tau_0;\tau_1]. \tag{24}$$

During stick the static friction $\mu(0)$ will increase in magnitude, until the maximum value μ_s is reached (cf. Figure 2(b)) and the mass starts to slip. Letting $\mu(0) = -\mu_s$ in equation (24) one finds the position at which the mass starts to slip:

$$x(\tau_1) = \gamma^2 \mu_s - 2\beta v_b. \tag{25}$$

When, at time $\tau = \tau_1$ the mass starts slipping again, the equation of motion (1) (with $a = 0$) then applies with $\dot{x} < v_b$. Hence the motion during slip is given by

$x(\tau) = u(\tau) + \bar{x}$, where u can be approximately determined by averaging as in section 3.2. For a first approximation it is assumed that u is given by equation (11) with a constant amplitude $A = A_1$ and phase $\theta = \theta_1$, so that

$$x(\tau) = A \sin(\tau + \theta_1) + \bar{x},$$
$$\dot{x}(\tau) = A_1 \cos(\tau + \theta_1), \quad \tau \in [\tau_1; \tau_2], \tag{26}$$

where $\bar{x}$ is the static equilibrium given by equation (7) and τ_2 is the time at which slipping stops. To determine the amplitude A_1 evaluate equation (26) for $\tau = \tau_1$, square and add to eliminate trigonometric terms, insert $\dot{x}(\tau_1) = v_b$ along with equations (25) and (7), and obtain

$$A_1 = \sqrt{v_b^2 + (\gamma^2(\mu_s - \mu(v_b)) - 2\beta v_b)^2}, \quad 0 \leqslant v_b < v_{b0} \tag{27}$$

or, using equation (5) to evaluate $\mu(v_b)$ and using equation (10)

$$A_1 = v_b \sqrt{1 + [\eta(1 - \tfrac{1}{3}(v_b/v_m)^2) - 2\beta]^2}, \quad 0 \leqslant v_b < v_{b0}. \tag{28}$$

Since the velocity of the mass must change continuously with time, the maximum and minimum displacements of the mass must occur during the slip phase; it cannot occur during stick because displacement here increases linearly with time. Hence, the amplitude A_1, determining displacements during the slip phase, also determines the oscillation amplitude of the complete stick–slip oscillation. So now one has an approximate simple expression for the stick–slip oscillation amplitude.

Whereas pure–slip oscillations occur at the natural frequency (equal to unity; cf. equation (1)) of the spring–mass system, stick–slip oscillations occur at a lower frequency ω_{ss},

$$\omega_{ss} = \frac{2\pi}{\tau_2 - \tau_0} = \frac{2\pi}{(\tau_2 - \tau_1) + (\tau_1 - \tau_0)}. \tag{29}$$

The lowering in frequency is not pronounced. For example, with parameters as for Figure 3, a Fourier analysis of numerical simulation results revealed a fundamental frequency of stick–slip oscillations of $\omega_{ss} \approx 0{\cdot}86$, and for v_b as small as 0·01 (where sticking occupies most of the oscillation period) ω_{ss} has dropped only to 0·83.

One can show that, for small damping β, the amplitude A_1 in equation (28) grows monotonically with the belt velocity v_b, attaining maximum value at the maximum v_b for which it is defined, $v_b = v_{b0}$. Hence the amplitude $A_{0,\max}$ as given by equation (22), occurring at the transition from pure-slip to stick–slip oscillations at $v_b = v_{b1}$, is the maximum attainable amplitude for the system.

3.4. SUMMARY AND ILLUSTRATION OF RESULTS (*NO* HARMONIC EXCITATION)

For small β and η and no harmonic excitation ($a = 0$ in equation (1)), self-excited oscillations can occur when $\eta > 2\beta$, that is, when the destabilizing effect of the

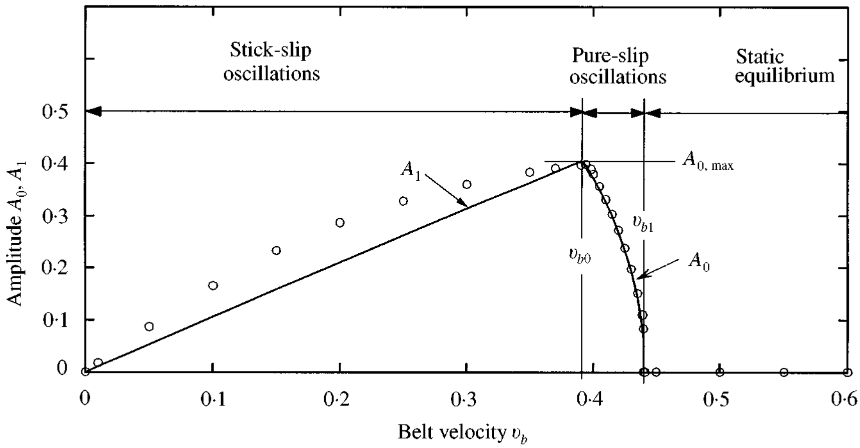

Figure 5. Amplitude of periodic motion of the mass as a function of velocity v_b when there is no harmonic excitation ($a = 0$) (——) Analytical prediction (equations (20) and (28); (○) numerical integration of equation (1). Parameters as given in the legend for Figure 3.

negative friction characteristic supersedes the stabilizing effect of viscous damping. The character of the response varies with belt velocity v_b as follows (v_{b0} and v_{b1} are the velocities defined by equations (19) and (21)):

(a) $v_b > v_{b1}$: Statical equilibrium, $x(\tau) = \bar{x} = \gamma^2\mu(v_b)$.
(b) $v_b \in [v_{b0}; v_{b1}]$: Pure-slip oscillations at a frequency near the natural frequency of the system, and amplitude A_0 increasing from zero at $v_b = v_{b0}$ to a maximum value $A_{0,max}$ at $v_b = v_{b1}$, as given by equations (20) and (22).
(c) $v_b \in [0; v_{b0}]$: Stick–slip oscillations at a frequency near or below the natural frequency of the system, and amplitude A_1 increasing from zero at $v_b = 0$ to a maximum value at $v_b = v_{b1}$, as given by equation (28).

Figure 5 compares the analytical predictions to results of numerical integration of equation (1). For the parameters of the figure one can use equations (21) and (19) to compute $v_{b0} \approx 0{\cdot}3944$ and $v_{b1} \approx 0{\cdot}4410$. For belt velocities between these two values, the mass performs pure-slip oscillations, as observed both from the numerical integration, and from the predictions of amplitude in equation (20) that gives excellent agreement. For $v_b > v_{b1}$ the constant-slip statical solution is stable, and there is no periodic motion. For $v_b < v_{b0}$ the mass performs stick–slip oscillations as predicted, though the analytical prediction (28) somewhat underestimates the true amplitude in the mid-range of $[0; v_{b1}]$ (this reflects the rather crude approximations made for predicting stick–slip oscillations).

Figure 6 shows response curves similar to that in Figure 5 for three levels of friction difference η. As observed, the agreement between analytical predictions and numerical simulation becomes better as η is decreased; this reflects that the analytical predictions assumes η to be small. The lower value of η in the figure is just above the critical value $\eta = 2\beta = 0{\cdot}10$, below which periodic motions cannot exist (cf. 20). Increasing η beyond the values of the figure, e.g., to $\eta \approx 1$, predictions of the onset and amplitude of pure-slip oscillations remains quite good, whereas

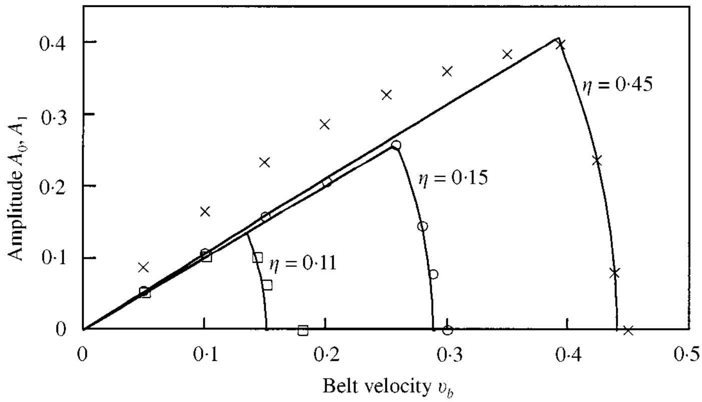

Figure 6. As Figure 5, but for varying levels of friction difference η. (——) Analytical prediction, ($\times$, $\bigcirc$, $\square$) numerical integration. Parameters as for Figures 3 and 5, but with $\mu_m = (0{\cdot}25, 0{\cdot}35, 0{\cdot}363333)$, giving $\eta = (0{\cdot}45, 0{\cdot}15, 0{\cdot}11)$ respectively (cf. equation (10)).

amplitudes of stick–slip oscillations becomes highly underestimated. Numerical simulation shows that for such large η the mass performs jerky periodic motions, the so-called relaxation oscillations (see e.g. reference [6]).

It appears that the amplitude of stick–slip oscillations increases almost linearly with belt velocity. Taylor-expanding equation (28) for small v_b, η and β, it is found that

$$A_1 = v_b + O(v_b \eta \beta), \quad 0 \leqslant v_b < v_{b0} \tag{30}$$

which for many cases (where v_b, η, and β are small) may serve as a good approximation.

So, it is possible to predict quite accurately the onset and the amplitude of self-excited oscillations for the model system (1) with no harmonic excitation—at least when the coefficients of static and dynamic friction or the difference between them are relatively small.

4. SELF-EXCITED OSCILLATIONS: CASE OF FAST HARMONIC EXCITATION

Next consider system (1) in the presence of harmonic excitation of small amplitude and very high frequency, that is, $a \ll 1$ and $\Omega \gg 1$. The primary question is how this excitation affects the existence and the character of self-excited oscillations, occurring at a much slower frequency ≈ 1 as discussed in section 3.

To examine this the method of direct partition of motions [17, 20–23] is used to separate slow and fast components of motions. This produces an autonomous differential equation for the slow motions, where the fast excitation is accounted for only by its "average" influence. The "slow" equation turns out to be in a form similar to equation (1) with $a = 0$, though with a changed form of μ, and so the results obtained in section 3 for that system can be reused here.

It also turns out that the effect of high-frequency excitation is to smoothen the discontinuity of the friction function. This opens a possibility of eliminating the negative slope of this function and thus to prevent the occurrence of self-excited oscillations.

4.1. SETTING UP AN EQUATION GOVERNING AVERAGED "SLOW" MOTIONS

4.1.1. *Separating fast and slow motions*

Consider obtaining approximate solutions to equation (1) for the case $\Omega \gg 1$ and $a \ll 1$. First equation (1) is written in the form

$$\ddot{x} + s(x, \dot{x}) = \Omega(a\Omega)\sin(\Omega\tau), \tag{31}$$

where s collects forces that do not explicitly depend on time,

$$s(x, \dot{x}) \equiv x + 2\beta\dot{x} + \gamma^2\mu(\dot{x} - v_b), \tag{32}$$

$a\Omega$ will be referred to as the *intensity* of the excitation, and its magnitude is assumed to be of the order of unity, $a\Omega = O(1)$. Assuming s to be similar or smaller in magnitude, $s \leqslant O(1)$, the excitation term on the right of equation (31) dominates the other terms in magnitude.

Then the total motion $x(\tau)$ of the mass is split into slow and fast components as follows:

$$x(\tau) = z(\tau) + \Omega^{-1}\varphi(\tau, \Omega\tau), \tag{33}$$

where z describes *slow motions* at the time-scale of free oscillations of the mass, and $\Omega^{-1}\varphi$ is an overlay of *fast motions* at the much faster rate of the external excitation. Perceive τ as the *slow time scale* and $\Omega\tau$ as a *fast scale*. The slow motions z are those of primary interest, whereas the details of the fast overlay φ interests us mainly by their effect on z.

Considering equation (33) as a transform of variables, from x to (z, φ), one needs to specify an additional constraint to make the transform unique. For this one requires that the "fast-time-average" of the fast motions be zero:

$$\langle\varphi(\tau, \Omega\tau)\rangle \equiv \frac{1}{2\pi}\int_0^{2\pi} \varphi(\tau, \Omega\tau)\,\mathrm{d}(\Omega\tau) = 0, \tag{34}$$

where $\langle\ \rangle$ defines time-averaging over one period of the fast excitation with the slow time τ considered fixed.

To determine the fast motions φ one substitutes equations (33) into (31), obtaining

$$\varphi'' = a\Omega\sin(\Omega\tau) - \Omega^{-1}(\ddot{z} + 2\dot{\varphi}' + s(z + \Omega^{-1}\varphi, \dot{z} + \varphi' + \Omega^{-1}\dot{\varphi})) - \Omega^{-2}\ddot{\varphi}, \tag{35}$$

where $\dot{z} = \mathrm{d}z/\mathrm{d}\tau$, $\dot{\varphi} = \partial\varphi/\partial\tau$, and $\varphi' = \partial\varphi/\partial(\Omega\tau)$. To the first order the stationary solution for φ is

$$\varphi(\tau, \Omega\tau) = -a\Omega\sin(\Omega\tau) + O(\Omega^{-1}), \tag{36}$$

where $O(\Omega^{-1})$ denotes small terms of the order Ω^{-1}. Hence, by equation (33) the total motion is

$$x(\tau) = z(\tau) - a\sin(\Omega\tau) + O(\Omega^{-2}). \tag{37}$$

To determine the slow motions z we average equation (35) and obtain, rearranging and using $\langle\varphi\rangle = 0$:

$$\ddot{z} + \langle s(z + \Omega^{-1}\varphi, \dot{z} + \varphi' + \Omega^{-1}\dot{\varphi})\rangle = 0 \tag{38}$$

or, substituting equation (36) for φ and dropping small terms of the order Ω^{-1} and higher:

$$\ddot{z} + \langle s(z - a\sin(\Omega\tau), \dot{z} - a\Omega\cos(\Omega\tau)\rangle = 0. \tag{39}$$

Substituting equation (32) for s one finds that the slow component of motion is governed by

$$\ddot{z} + 2\beta\dot{z} + z + \gamma^2\bar{\mu}(\dot{z} - v_b) = 0, \tag{40}$$

where $\bar{\mu}$ defines the *effective friction characteristic* in the presence of fast excitation:

$$\bar{\mu}(v_r) \equiv \langle\mu(v_r - a\Omega\cos(\Omega\tau))\rangle. \tag{41}$$

Equation (40) for the slow motions is similar in form to equation (1) for the total motion, though, with the time-dependent excitation accounted for by the effective friction characteristic $\bar{\mu}$ instead of the ordinary μ. Equation (40) is autonomous, and thus is much easier to solve than the non-autonomous equation (1).

As for the initial conditions for the equation for slow motions (40) one finds, using equation (37) and neglecting terms of order Ω^{-2} and smaller that

$$z(0) = x(0), \qquad \dot{z}(0) = \dot{x}(0) + a\Omega. \tag{42}$$

Then equations (40)–(42) constitute the resulting differential equation for slow motions z of the mass.

4.1.2. *Calculating the effective friction characteristic*

Now turn to determining $\bar{\mu}$ for the specific μ given by equation (5). For this equation (5) is rewritten as

$$\mu(v_r) = \mu_s\,\mathrm{sgn}(v_r) + \alpha_1 v_r + \alpha_3 v_r^3, \tag{43}$$

where

$$\alpha_0 \equiv \mu_s, \qquad \alpha_1 \equiv -\tfrac{3}{2}(\mu_s - \mu_m)/v_m, \qquad \alpha_3 \equiv \tfrac{1}{2}(\mu_s - \mu_m)/v_m^3. \tag{44}$$

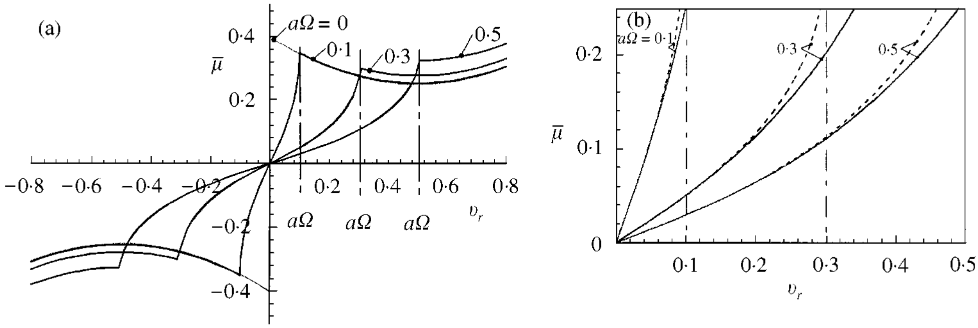

Figure 7. (a) Effective friction characteristic $\bar{\mu}(v_r)$ as given by equation (47) for different intensities $a\Omega$ of fast excitation (parameters as for Figure 4). Fast excitation smoothness the characteristic, at sufficiently large intensity canceling the negative slope. (b) Initial part of the friction–velocity characteristic: (– – –) using equation (47) as in figure (a); (——) using third order Taylor expansion (48)–(49).

For calculating the average term in equation (41) note that if $|v_r| > a\Omega$ then $v_r - a\Omega\cos(\Omega\tau)$ has constant sign for all $\Omega\tau$, whereas if $|v_r| \leqslant a\Omega$ then

$$v_r - a\Omega\cos(\Omega\tau)\begin{cases} \geqslant 0 & \text{for } \Omega\tau \in [\Omega\tau_1;\Omega\tau_2], \\ \leqslant 0 & \text{for } \Omega\tau \in [0;\Omega\tau_1] \cup [\Omega\tau_2;2\pi], \end{cases} \tag{45}$$

where

$$\Omega\tau_1 = \arccos(v_r/a\Omega), \qquad \Omega\tau_2 = 2\pi - \Omega\tau_1. \tag{46}$$

Using this and equation (43) and the definition of $\langle\ \rangle$ in equation (34) the average in equation (41) after some trivial integrations and rearrangements becomes

$$\bar{\mu}(v_r) = \begin{cases} \alpha_0(1 - \frac{2}{\pi}\arccos(v_r/(a\Omega))) + (\alpha_1 + \frac{3}{2}\alpha_3(a\Omega)^2)v_r + \alpha_3 v_r^3 & \text{for } |v_r| \leqslant a\Omega, \\ \mu(v_r) + \frac{3}{2}\alpha_3(a\Omega)^2 v_r & \text{for } |v_r| \geqslant a\Omega. \end{cases} \tag{47}$$

Figure 7(a) depicts this effective friction characteristic for different intensities $a\Omega$ of fast excitation. It appears that the fast excitation effectively changes the friction characteristic in two ways: (1) For relative velocities $|v_r| \leqslant a\Omega$ the discontinuity at $v_r = 0$ is smoothened; and (2) for $|v_r| > a\Omega$ the effective friction coefficient is larger than the "true" friction coefficient. The first effect may effectively cancel the negative slope of the friction characteristic, and thus prevent self-excited oscillations.

4.1.3. *Further simplifications*: *effective friction characteristic in polynomial form*

Taylor-expanding equation (47) for small v_r, it is found that

$$\bar{\mu}(v_r) = \hat{\alpha}_1 v_r + \hat{\alpha}_3 v_r^3 + O(v_r^5) \quad \text{for } |v_r| \leqslant a\Omega, \tag{48}$$

where

$$\hat{\alpha}_1 \equiv \frac{2\alpha_0}{\pi a\Omega} + \alpha_1 + \tfrac{3}{2}\,\alpha_3(a\Omega)^2, \qquad \hat{\alpha}_3 \equiv \alpha_3 + \frac{\alpha_0}{3\pi(a\Omega)^3} \tag{49}$$

or, in terms of original variables (cf. equation (44)):

$$\hat{\alpha}_1 = \frac{2}{\pi}\frac{\mu_s}{a\Omega} + \frac{3}{2}\frac{\mu_s - \mu_m}{v_m}\left(\frac{1}{2}\left(\frac{a\Omega}{v_m}\right)^2 - 1\right) \qquad \hat{\alpha}_3 = \frac{\mu_s}{3\pi(a\Omega)^3} + \frac{(\mu_s - \mu_m)}{2v_m^3}. \tag{50}$$

To the third order the polynomial (48) provides a reasonable approximation to the averaged friction characteristic for $|v_r| < a\Omega$, as appears from Figure 7(b).

The first term in equation (48) is linear in the velocity, so $\hat{\alpha}_1$ can be said to represent an *effective viscous damping coefficient*. Here the first term describing $\hat{\alpha}_1$ in equation (50) may be recognized as the equivalent viscous damping coefficient for an object with simple Coulomb friction (i.e., $\mu_s = \mu_m$) in contact with a rapidly vibrating plane [17]. This coefficient approaches zero as the intensity of vibration $a\Omega$ is increased. The second term describing $\hat{\alpha}_1$ represents the effect of non-constant friction coefficient present when $\mu_s > \mu_m$; this term *in*creases with the vibration intensity $a\Omega$. So, the two terms of $\hat{\alpha}_1$ combine to an effective damping coefficient that drops steeply from infinity at intensity $a\Omega = 0$ to a minimum value at $(a\Omega)^3 = 4/(3\pi(1 - \mu_m/\mu_s))$, and then again increases for higher intensities.

One can show that when the difference in friction coefficients $\mu_s - \mu_m$ is not very large, as assumed in this study, then the smoothened friction characteristic (48) is a monotonically increasing function of v_r, i.e., it has positive slope everywhere.

Summing up, the effective friction characteristic in the presence of fast vibrations is given by equation (47). However, for $|v_r| \leqslant a\Omega$ one can use the more simple expression (48) with reasonable accuracy.

4.1.4. *Checking and Illustrating Results*

In Figure 8, part of the time series $x(\tau)$ from Figure 4 is shown again along with the corresponding solution $z(\tau)$ to the equation of slow motions (40) with $\bar{\mu}$ given by equation (47). As observed the slow component z traces the moving fast-time-average of the full motion x, as it should. Also, according to equation (37) the amplitude of the fast component of motion should be equal to the amplitude a of the excitation ($=0{\cdot}01$ for Figure 8), and the amplitude of the fast component of velocity should be $a\Omega$ ($= 0{\cdot}5$ for the figure); both quantities are confirmed by Figure 8.

Hence, for examining the response of the present system to fast harmonic excitation, the approximate solutions given by equation (37) with equations (40) and (47) are considered rather than the full equation of motion (1).

4.2. SELF-EXCITED OSCILLATIONS (WHEN THERE IS FAST HARMONIC EXCITATION)

Consider the conditions for self-excited oscillations in the presence of fast harmonic excitation, $a \neq 0$. For this equation (40) governing slow motions z of the system is used. This equation is identical in form to equation (1) with $a = 0$, which was examined in section 3. Hence one can reuse the results obtained there, replacing the "true" friction characteristic $\mu(v_r)$ with the effective friction characteristic $\bar{\mu}(v_r)$ given by equation (47) (or equation (48) for small v_r).

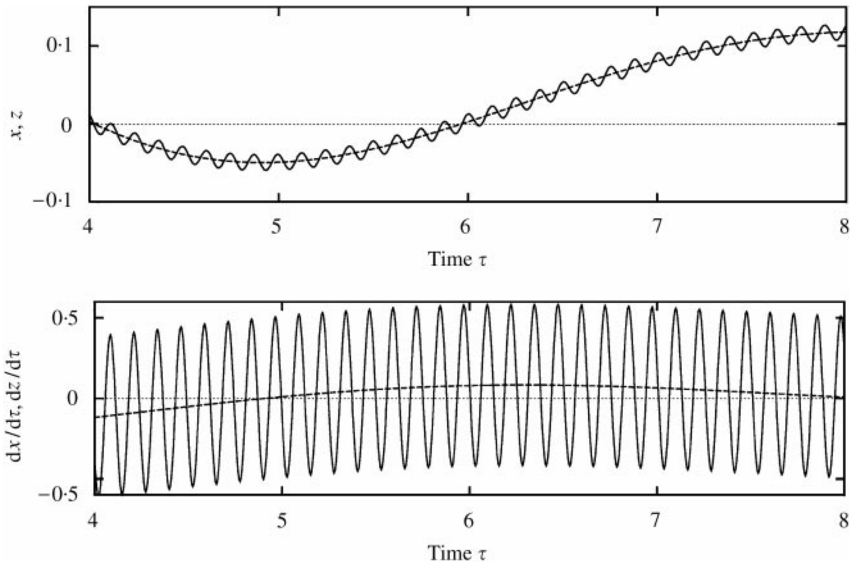

Figure 8. System responses in the presence of fast harmonic excitation (parameters as for Figure 4). (——) Full motion $x(\tau)$ by numerical integration of equation (1); (– – –) slow component of motion $z(\tau)$ by numerical integration of equation (40) with $\bar{\mu}$ given by equation (47). The slow component traces the moving fast-time-average of the full motion.

The equation of slow motion (40) has a static equilibrium at $z = \bar{z}$,

$$\bar{z} = -\gamma^2 \bar{\mu}(-v_b) = \gamma^2 \bar{\mu}(v_b) \tag{51}$$

since then $\ddot{z} = \dot{z} = 0$. This is called a *quasi-equilibrium*, because the mass is actually not at rest here; it performs vibrations at very small amplitude a and high frequency Ω (cf. equation (37)).

In section 3.2, for $a = 0$ it was shown that the equilibrium $x = \bar{x}$ becomes unstable and self-excited oscillations occur when the slope of μ at v_b is more negative than a threshold value determined by the damping, $\mu'(v_b) + 2\beta/\gamma^2 < 0$ (cf. equation (17)). Then, similarly, for $a \neq 0$ the (quasi-)equilibrium $z = \bar{z}$ becomes unstable and self-excited oscillations appear when

$$\bar{\mu}'(v_b) + 2\beta/\gamma^2 < 0. \tag{52}$$

So, we should examine the slope of $\bar{\mu}(v_b)$, where $\bar{\mu}$ is given by equation (47) and illustrated for typical parameters in Figure 7.

In this study the friction coefficients μ_m and μ_s are assumed not for differ very much in magnitude. Then the first part of $\bar{\mu}(v_r)$ (for $|v_r| \leqslant a\Omega$) has positive slope everywhere (one can show that negative slope cannot occur as long as $\mu_m/\mu_s > 1 - \sqrt{6}/\pi \approx 0{\cdot}22$). Consequently, with high-frequency excitation of intensity $a\Omega$, self-excited oscillations cannot occur for belt velocities $v_b \leqslant a\Omega$.

For the second part of $\bar{\mu}(v_r)$ (for $|v_r| \geqslant a\Omega$) one finds, using equations (47) and (44), that the slope is

$$\bar{\mu}'(v_b) = \mu'(v_b) + \tfrac{3}{4}(a\Omega)^2\,(\mu_s - \mu_m)/v_m^3 \quad \text{for } v_b \geqslant a\Omega \tag{53}$$

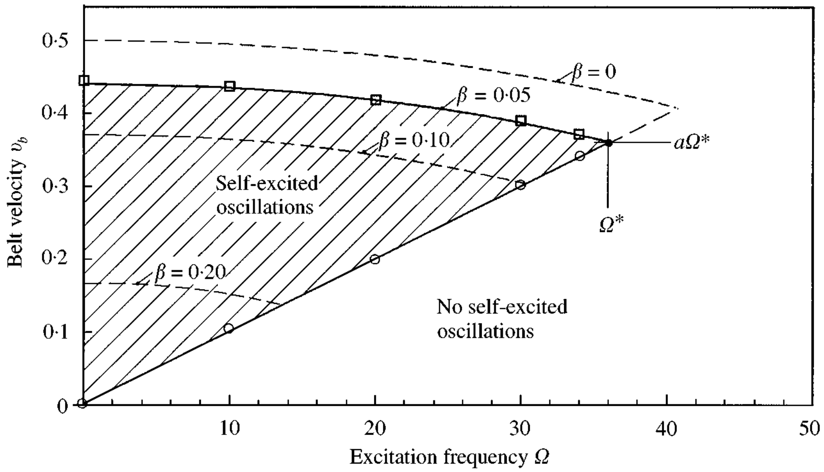

Figure 9. Ranges of belt velocities producing self-excited oscillations, as function of excitation frequency. (—, - - - -) Analytical prediction (equation (55)); (□, ○) numerical simulation (equations (1) and (6)) ($a = 0{\cdot}01$; other parameters as given in the legend of Figure 4).

so that condition (52) is fulfilled when

$$\mu'(v_b) + \tfrac{3}{4}(a\Omega)^2(\mu_s - \mu_m)/v_m^3 + 2\beta/\gamma^2 < 0, \quad v_b \geqslant a\Omega \tag{54}$$

or, using equations (5) and (10) and rearranging:

$$a\Omega \leqslant v_b < v_m\sqrt{1 - \tfrac{1}{2}(a\Omega/v_m)^2 - 2\beta/\eta}\,. \tag{55}$$

It appears there is a certain range of belt velocities where self-excited oscillations can occur. When $a\Omega = 0$ the expression gives the range already obtained in section 3 (cf. equation (19)). As $a\Omega$ is increased the range is reduced in width, vanishing at $a\Omega = a\Omega^*$ where

$$a\Omega^* = \sqrt{\tfrac{2}{3}}v_m\sqrt{1 - 2\beta/\eta}\,. \tag{56}$$

Hence when $a\Omega > a\Omega^*$ self-excited oscillations cannot exist for any value of belt velocity v_b.

Figure 9 illustrates these relationships for typical values of system parameters. As it appears the agreement with results of numerical simulation is very good. The figure also shows how increased damping β decreases the range of belt velocities where self-excited oscillations occur, and decrease the excitation frequency needed to quench such oscillations.

The amplitude of self-excited oscillations can be calculated by using perturbation analysis, as in section 3 for the case $a = 0$. Rather than doing that, one notes that the square of oscillation amplitudes will be proportional to the negative slope of $\bar{\mu}(v_b)$ divided by the coefficient of the cubic term of the Taylor expansion of $\bar{\mu}(v_b)$ (as in the expression for A_0 in equation (16)). Further, as mentioned above, self-excited oscillations can occur only in a range of belt velocities beyond $a\Omega$; hence to calculate slopes and cubic coefficients we should use the second part of equation (47), valid for $|v_r| \geqslant a\Omega$. Then, as noted from equation (47), the cubic coefficient of

$\bar{\mu}$ is the same as that for μ, whereas the slope is less negative (being increased by the positive number $3/2\alpha_3(a\Omega)^2$). Consequently, *if* self-excited oscillations occur in the presence of high-frequency excitation, then their amplitude will be less than without this excitation.

Summing up, one may say that high-frequency excitation of intensity $a\Omega > a\Omega^*$ prevents self-excited oscillations at all belt velocities v_b, whereas when $a\Omega < a\Omega^*$ self-excited oscillations are confined to occur only at a certain range of belt velocities (given by equation (55)).

5. QUENCHING SELF-EXCITED VIBRATIONS

By the results of section 3 and 4 one can now sum up on the possibilities of quenching friction-induced oscillations for the model considered.

5.1. BY APPLYING MORE DAMPING OR CHOOSING A DIFFERENT FRICTION MATERIAL

According to section 3.4, if $2\beta > \eta = 3/2\ \gamma^2(\mu_s - \mu_m)/v_m$, then $v_{b0} = v_{b1} = 0$. Under this condition the statical equilibrium is always stable, and self-excited oscillations cannot occur at any value of belt velocity v_b. Hence friction-induced oscillations can be eliminated by increasing the amount of viscous damping β. Alternatively, one can use a material with smaller difference between static and kinetic friction, $\mu_s - \mu_m < 4/3\beta v_m/\gamma^2$, or lubrication can be applied to reduce μ_s and μ_m to sufficiently low levels.

It may not be feasible to choose parameters that will completely suppress self-excited oscillations. Still, increasing β or decreasing μ_s, μ_m, or $\mu_s - \mu_m$ will reduce the maximum amplitude $A_{0,max}$ of self-excited oscillations, as well as the range$]0; v_{b1}]$ of velocities where they occur; cf. equations (22), (19), and Figure 6.

5.2. BY USING FAST VIBRATIONS

As described in section 4.2 and illustrated by Figure 9, self-excited oscillations are totally eliminated if $a\Omega > a\Omega^*$, where $a\Omega$ is the intensity of the fast vibrations, and $a\Omega^*$ is the simple function of system parameters given by equation (56). For small damping β one has $a\Omega^* \approx 0{\cdot}8v_m$, i.e., to quench self-excited oscillations it will be *sufficient* to use excitation having intensity equal to the (non-dimensional) velocity corresponding to the minimum kinetic coefficient of friction. The presence of viscous damping β will aid in reducing the requirement for external excitation, as quantified by equation (56).

Whereas $a\Omega > a\Omega^*$ is a sufficient condition for preventing self-excited oscillations, one can set up *necessary* conditions that are less demanding. For example, the necessary condition for quenching self-excited oscillations occurring at a specified operating speed $v_b = \hat{v}_b$ is (cf. equations (55), (56), and Figure 9)

$$a\Omega > \begin{cases} \hat{v}_b & \text{for } \hat{v}_b \leqslant a\Omega^*, \\ \sqrt{3(a\Omega^*)^2 - 2\hat{v}_b^2} & \text{for } \hat{v}_b > a\Omega^*. \end{cases} \tag{57}$$

On the other hand, the conditions for quenching oscillations occurring at belt speeds *below* a certain value $\hat{v}_b$ is

$$a\Omega > \begin{cases} \hat{v}_b & \text{for } \hat{v}_b \leqslant a\Omega^*, \\ a\Omega^* & \text{for } \hat{v}_b > a\Omega^*. \end{cases} \tag{58}$$

Similar conditions can easily be set up for other cases, e.g., quenching self-excited oscillations occurring at belt speeds *above* a certain value, or speeds within a specified *range*.

5.3. ENERGY CONSIDERATIONS

How much energy is required to quench self-excited oscillations this way?

Assume that the intensity of fast excitation is fixed at $a\Omega = a\Omega^*$, so that self-excited oscillations are prevented at all belt speeds (cf. equation (56) and Figure 9); then the mass is at a state of quasi-equilibrium ($\dot{z} = 0$) and by equation (37) one has $\dot{x} = -a\Omega \sin(\Omega\tau) + O(\Omega^{-1})$. Inserting this into equation (4) and neglecting terms that are small when $\Omega \gg 1$, one finds that the energy required for quenching self-excited oscillations is

$$E^*_{inp} = \tfrac{1}{2}(a\Omega^*)^2 \cos^2(\Omega\tau) = \tfrac{1}{3} v_m^2 (1 - 2\beta/\eta) \cos^2(\Omega\tau). \tag{59}$$

This can be compared, e.g., to the kinetic energy of the strongest self-excited oscillations that would occur if the fast harmonic excitation was not there ($a = 0$). Using equation (4) and the results of sections 3.1 and 3.2 one finds

$$E^*_{kin} = \tfrac{1}{2} A^2_{0,max} \cos^2(\tau + \theta_0) = \tfrac{2}{5} v_m^2 (1 - 2\beta/\eta) \cos^2(\tau + \theta_0) \tag{60}$$

and the ratio of energy levels become

$$\frac{\max(E^*_{inp})}{\max(E^*_{kin})} = \left(\frac{a\Omega^*}{A_{0,max}}\right)^2 = \frac{5}{6} \tag{61}$$

Thus, the energy required for quenching self-excited oscillations by using fast vibrations is always less than the kinetic energy of the self-excited oscillations.

5.4. DISCUSSION

Fast vibrations quench self-excited oscillations by changing the effective friction properties of a system. Of course this may spoil proper functioning of a device that specifically relies on friction. For example, for a disk or drum break the squeal may decrease or cease, but so may the maximum braking force. Then adjusting the intensity of fast excitation as a function of sliding velocity could be considered. It might be possible to keep $a\Omega$ slightly larger than v_b, i.e., to let a controller adjust the vibration intensity in closed loop with measurements of the velocity. Then the friction force would be kept at a level similar to that without fast excitation (in fact even larger, cf. Figure 7(a)), while there would be no self-excited oscillations.

To use high-frequency excitation in the manner described here, there are costs to pay in the form of extra devices, energy, complexity, and possibly new problems. It should be recalled that the technique does not simply turn self-excited oscillations into absolute rest, but rather "transform" them into small-amplitude vibrations at very high frequency (see Krylov and Sorokin [24] for a similar observation in a related context). If this frequency is outside the audible range then one problem might be solved; however, the vibrations can be quite energetic and may thus introduce other problems, e.g., heat generation.

It might be possible to draw energy for the high-frequency excitation from the system itself, rather than providing it externally. For example, surface roughness having a space-periodic character is mathematically equivalent to time-periodic excitation [11, 25]. However, this kind of excitation is not easily controlled.

6. CONCLUSIONS

This work provides a theoretical basis for understanding how friction-induced oscillations are affected by external high-frequency excitation. For the traditional mass-on-moving-belt model, simple analytical expressions are given for predicting the occurrence of self-excited oscillations with and without this excitation. According to these, high-frequency excitation can effectively cancel the negative slope in the friction–velocity relationship, and may thus prevent self-excited oscillations from occurring. To accomplish this it is sufficient that the (non-dimensional) product of excitation amplitude and frequency exceed the velocity corresponding to the minimum kinetic coefficient of friction. Simple expressions are given also for predicting the excitation necessary for quenching self-excited oscillations at or below a specified belt velocity. These and other results contribute to the general understanding of how friction properties may change under the action of fast vibrations.

High-frequency excitation effectively turns dry friction into a viscous-like form of damping, similar to the kind of dissipation that would occur when using lubricating oil. Unlike lubrication, however, the damping effect created by fast vibrations can be controlled very quickly, and can easily be removed if unwanted. One could consider designing a controller that just prevents friction-induced vibration from growing, without interferring significantly with the dry friction properties of the controlled device.

This work focuses on understanding, predicting, and quantifying on a purely theoretical level the effects of high-frequency excitation on friction-induced oscillations. The quite simple expressions (55) and (56) for predicting the occurrence of self-excited oscillations in the presence of high-frequency excitation has been developed using a great deal of approximation. Nevertheless, as seen in Figure 9, they seem to reproduce very accurately the results of numerical simulation of the original full equations of motions. Hence, they can be used for designing and evaluating laboratory experiments concerning the phenomenon under study. The results call for experimental support.

REFERENCES

1. J. W. S. Rayleigh 1877 *The Theory of Sound*. New York: Dover Publications (second edition 1945 re-issue).

2. P. DEN HARTOG 1984 *Mechanical Vibrations*. New York: Dover Publications.
3. S. YANG and R. F. GIBSON 1997 *International Journal of Materials and Product Technology* **12**, 496–513. Brake vibration and noise: reviews, comments and proposals.
4. Y. G. PANOVKO and I. I. GUBANOVA 1965 *Stability and Oscillations of Elastic Systems, Paradoxes, Fallacies and New Concepts*. New York: Consultants Bureau.
5. TONDL 1991 *Quenching of Self-excited Vibrations*. Amsterdam: Elsevier.
6. H. NAYFEH and D. T. MOOK 1979 *Nonlinear Oscillations*. New York: Wiley.
7. YU. A. MITROPOLSKII and V. D. NGUYEN 1997 *Applied Asymptotic Methods in Nonlinear Oscillations*. Dorderecht: Kluwer.
8. K. POPP 1992 *Friction-Induced Vibration, Chatter, Squeal, and Chaos*, ASME DE **49**, 1–12. Some model problems showing stick-slip motion and chaos.
9. M. YOKOI and M. NAKAI 1979 *Bulletin of the JSME* **22**, 1665–1671. A fundamental study on frictional noise (1st Report, the generating mechanism of rubbing noise and squeal noise).
10. M. YOKOI and M. NAKAI 1981 *Bulletin of the JSME* **24**, 1470–1476. A fundamental study on frictional noise (3rd Report, the influence of periodic surface roughness on frictional noise).
11. R. A. IBRAHIM 1992 *Friction-Induced Vibration, Chatter, Squeal, and Chaos*, ASME DE **49**, 107–121. Friction-induced vibration, chatter, squeal, and chaos: Part I—mechanics of friction.
12. R. A. IBRAHIM 1992 *Friction-Induced Vibration, Chatter, Squeal, and Chaos*, ASME DE **49**, 107–121. Friction-induced vibration, chatter, squeal, and chaos: Part II—dynamics and modelling.
13. J. MCMILLAN 1997 *Journal of Sound and Vibration* **205**, 323–335. A non-linear friction model for self-excited vibrations.
14. K. POPP, N. HINRICHS, and M. OESTREICH 1996 *Dynamics with Friction. Modeling, Analysis and Experiment—Part I* (A. Guran, F. Pfeiffer and K. Popp, editors). Singapore. World Scientific. Analysis of a self-excited friction oscillator with external excitation.
15. N. HINRICHS, M. OESTREICH and K. POPP, 1998 *Journal of Sound and Vibration* **216**, 435–459. On the modelling of friction oscillators.
16. F.-J. ELMER 1997 *Journal of Physics A* **30**, 6057–6063. Nonlinear dynamics of dry friction.
17. I. I. BLEKHMAN 1994 *Vibrational Mechanics*. Moscow:Fizmatlit Publishing Company. (In Russian. To appear in English translation by World Scientific Publishing Company, 1999).
18. M. OESTREICH, N. HINRICHS and K. POPP, 1996 *Archive of Applied Mechanics* **66**, 301–314. Bifurcation and stability for a non-smooth friction oscillator.
19. J. J. THOMSEN 1997 *Vibrations and Stability, Order and Chaos*. London: McGraw-Hill.
20. I. I. BLEKHMAN 1999 'Forming the properties of nonlinear mechanical systems by means of vibration, *DCAMM Report* 616, Technical University of Denmark, Lyngby.
21. J. S. JENSEN 1998 *Journal of Sound and Vibration* **215**, 125–142. Non-linear dynamics of the follower-loaded double pendulum with added support-excitation.
21. J. S. JENSEN 1999 *DCAMM Report S* 83 (*Ph.D. thesis*), *Technical University of Denmark, Lyngby*. Non-Trivial Effects of Fast Harmonic Excitation.
23. J. J. THOMSEN 1999 *Proceedings of the IUTAM/IFToMM Symposium on Synthesis of nonlinear Dynamical Systems— SNDS* '98, Riga, Latvia, August 24–28, 1998, Dordrecht: Klüwer Academic Press. Vibration-induced displacement using high-frequency resonators and friction layers. (to appear).
24. V. KRYLOV and S. V. SOROKIN 1997 *Smart Materials and Structures* **6**, 573–582. Dynamics of elastic beams with controlled distributed stiffness parameters.
25. M. NAKAI and M. YOKOI 1990 Japan *Journal of Tribology* **35**, 513–522. Generation mechanism of friction noises in dry friction.